FINITE ELEMENT MODEL OF THE LIVER FOR COMPUTER-ASSISTED HEPATIC TUMOR ABLATION

A. Leroy[1], Y. Payan[1], D. Voirin[1,2], C. Létoublon[2] and J. Troccaz[1]

1. ABSTRACT

Radiofrequency tumor ablation requires precise localization of the carcinoma. In a first step, a procedure for computer-assisted puncture guiding has been assessed. Intra-operative tracking of liver movements is not easy, since the structure not only moves during intervention, but also deforms. Therefore, a 3D biomechanical model has been developed to quantify liver deformations under various constraints. This model is made of 7 hepatic segments, Glisson's capsule and tumors. By applying surfacic constraints, the pressure of a needle and the breathing movements have been simulated, and the resulting tumor movements quantified.

2. INTRODUCTION

Radiofrequency ablation is a brand new technique to eradicate metastatic malignancies confined to the liver. It consists in inserting a radiofrequency needle percutaneously through the liver parenchyma and to the tumor, which is eventually burnt [1]. Therefore, a critical factor for the deletion of the tumor and for the patient's survival is the accuracy of the localization. This represents a great challenge, as the liver not only moves, but also deforms during intervention.
Previous works have been achieved in Computer Assisted Surgery, mainly applied to bony structures. Volume segmentation, pre-operative planning, intra-operative registration, and finally trajectory guiding were relatively easy to implement, as the targeted anatomical structures (a vertebra for instance) were of course rigid [2].
Preliminary studies have been carried out to assess the feasibility of a computer-assisted

Keywords: liver, radiofrequency, FEM, surfacic constraints, motion tracking.

[1] Laboratoire TIMC - Faculté de Médecine - Domaine de la Merci- 38706 La Tronche cedex - France
[2] Service de chirurgie générale et digestive – CHU de Grenoble
BP 217 – 38043 Grenoble cedex 9 - France

surgery system for the liver [3]. In a second step, which is the object of this article, the task consisted in assessing the movements of the liver and its deformations under various constraints. A finite element model and some software tools were developed for that purpose.
After building the finite element model of the liver out of MRI slices, anatomical structures were added to it for more realism, and biomechanical parameters were fixed for each structure, according to in vivo and in vitro measurements [4] and [5]. Surfacic constraints representing the contact with the surrounding organs, as well as time-dependent boundary conditions were then defined to carry out simulations in order to assess the movements of the tumors.
This article is organized as follows. Part 3 presents the construction steps of the model, while part 4 deals with validation and simulation experiments on that model.

3. MODEL CONSTRUCTION

3.1 Shape and Volume

The shape of the model was extracted out of manually segmented MRI slices. The ANSYS™ meshing tool then filled the so-created volume with 18132 tetrahedrons.

3.2 Anatomical Structures

In order to complete this FE volume, several anatomical structures have been added to the model. First, seven hepatic segments were delimited with the help of a surgeon (fig.1). Then, in each segment, a few elements were chosen to represent a tumor (fig.2). Finally, Glisson's capsule, which is a thin capsule covering the hepatic parenchyma, and which plays an important role in the rigidity of the liver, was extruded out of the surface (8929 wedge elements) (fig.3).

fig.1 – The 7 hepatic segments

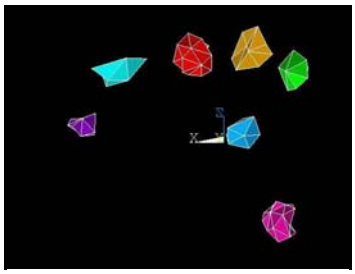

fig.2 – 7 hepatic tumors

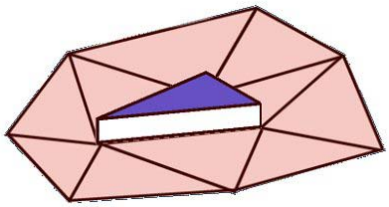

fig.3 – A wedge element from Glisson's capsule

3.3 Mechanical Properties

Once the geometry of the model is defined, mechanical properties should be set in each structure. All material are isotropic. Young moduli for the parenchyma and for Glisson's capsule were found in literature [4] and [5], and summarized in fig.4.

	E (kPa)	**ν**
Parenchyma	5	0.49
Tumors	50	0.49
Glisson's capsule	400	0.49

fig.4 – The rheological properties given to our model

On that subject, one may notice that Fiona Carter [5] carried out indentation tests on living porcine as well as on human patients, whereas Diane Dan [4] studied in vitro liver pieces. We actually trusted Dan's measures, assuming that the rheology that we need is that of an unconstrained liver. We

have modeled surfacic constraints ourselves, indeed (see 3.4). On the contrary, an in vivo liver is naturally constrained by the surrounding organs and thus, in a sense, more rigid.
The Poisson ratio of all structures is set to 0.49, as the liver, mainly filled with water, is quasi incompressible.
Setting the rheology in the liver model is a crucial step in its definition. Some validation tests will be presented in 4.1.

3.4 Static Surfacic Constraints

The liver is constrained inside the abdomen by the surrounding anatomical structures.
The ribs are a rigid barrier that prevent the liver from moving towards its anterior, lateral, and posterior-right faces. To model this constraint, the surfacic nodes are forced to move in their tangential plane (in fig.5: the area in contact with the anterior ribs).

fig.5 – The anterior face constrained by the ribs

The liver is attached to the diaphragm on its superior face, by the triangular ligaments. Those ligaments are rigid enough for the liver to follow the periodic movements of the diaphragm. The displacements of the superior nodes are thus controlled by breathing.

3.5 Dynamic Surfacic Constraints

The liver is also in contact with other soft, moving organs, such as the right kidney, the stomach, and the colon. Such barriers can constrain the liver only to a certain extent ; in fact, their reaction to the liver motion is somehow proportional to that motion.
The surfacic constraint is modeled by normal forces applied to the nodes in the contact areas. Their value is proportional to the inverse distance of the liver surface to an unreachable limit (eq.1), located a few centimeters away in the normal direction, and corresponding to a virtual anatomical boundary (fig.6).

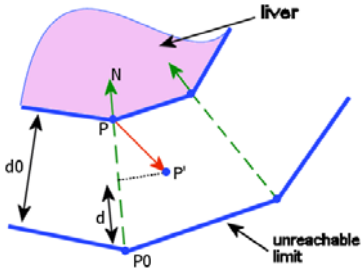

fig.6 – Dynamic constraint modelization

$$\vec{F} = f(d) \cdot \vec{N}$$

$$f(d) = \frac{f_0(d_0 - d)}{d^k}, k \in \mathbb{R} \quad \text{if } d < d_0 \qquad \textbf{(eq.1)}$$
$$= 0 \qquad \text{otherwise}$$

The f_0 and d_0 parameters depend on the organ. The kidney is much more rigid than the liver, whereas the colon and the stomach are much softer. Those differences are thus modelized by the intensity of the feedback force.

4. EXPERIMENTS AND RESULTS

4.1 Model Validation

Our first concern was to validate the mechanical properties given to the liver.

Both in vivo and in vitro indentation measures were available, and the latter was chosen (see 3.3). In a first step, that choice had to be validated. After a tumorectomy at the hospital, the surgeon allowed us to carry out a simple indentation test on the ablated liver portion (fig.7). That piece was roughly a 15mm-high cylinder that contained a small carcinoma. We assumed that most of the portion was made of healthy tissue. The experiment consisted in putting a 100g mass on the portion, measuring its deformation, and then calculating the Young modulus. We found E=4.2 kPa, which is not far from the minimal value 2.2kPa proposed by Ottensmeyer [6].

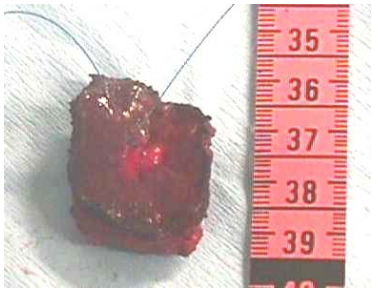

fig.7 – The ablated cylindrical liver portion

Inversely, the same experiment was done on a cylinder meshed under ANSYS™, quasi-incompressible and with the same elasticity as previously measured. Qualitatively, the observed deformation is similar to that of the liver portion (a third of the height, ie 5mm, cf fig.8 and fig.9)

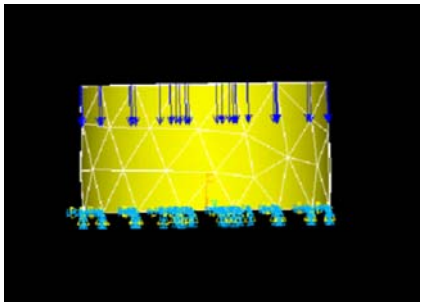

fig.8 – Simulation of the compression experiment: 100g applied on the superior face

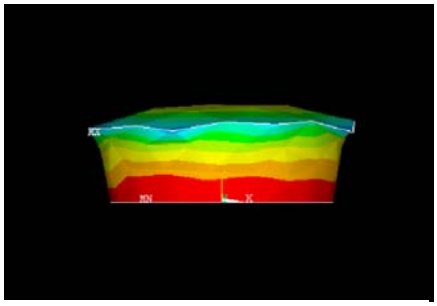

fig.9 – The result of the simulation

The other experiment consisted in applying some surfacic pressures to the model, while setting both static and dynamic constraints. During that indentation test, forces ranging from 0.05N to 2N were applied on a 17mm² area, on the 8th hepatic segment. The results of the test match rather well Carter's figures (fig.10), when confined to the "small displacements" interval. One can notice that the blue force/displacement curve is linear, since the solutions were processed in linear mode.

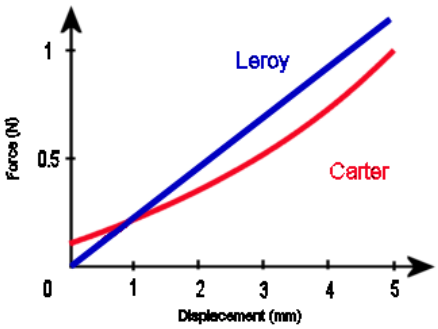

fig.10 – Force/Displacement curves based on indentation tests on a sheep (Carter) and on our model (Leroy)

4.2 Needle Pressure Simulation

The penetration of the needle in the parenchyma and its progression were not modelized in this study. The action of the needle was just approximated by moving one of the surface nodes 10mm in the direction of the tumor (that displacement of the surface is

due to the penetration of the needle, which is up to 3.5mm thick, through Glisson's capsule).

Once the target is located in one of the 7 segments of the liver, one has to decide in which segment to insert the needle to reach the target. Out of the 7x7=49 possible "segment-tumor" directions, we defined 12 of them with the help of a surgeon. The question was then, what direction to choose among these to prevent the targeted tumor from moving too much, and thus from making the surgical action inaccurate and of limited therapeutic efficiency.

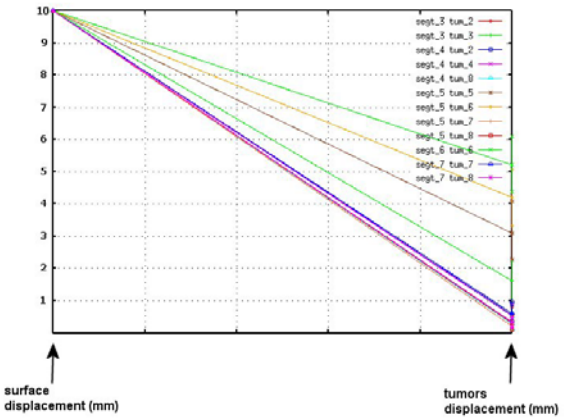

fig.11 – 12 pressure simulations between a segment and a tumor. On the right axis, the displacements of the tumors.

The graph in fig.11 shows on its left Y-axis the 10mm-penetration of the needle through the surface, and on its right Y-axis, the movement of the targeted tumors. Each colored line represents one of the 12 privileged directions. All surfacic constraints have been applied to process those simulations, and the diaphragm was maintained fixed.

One can see that most of the tumors have an infra-millimetric movement, but four of them may move up to 5mm away from their initial position. 5mm is a displacement that should not be neglected in future investigations in radiofrequency ablation [7].

4.3 Breathing Simulation

The second aspect of the study consists in measuring the global motion of the liver, as well as tumors displacements, during breathing. Such measures on human liver can be found in [8] and [9].

The diaphragm is the main muscle involved in the breathing mechanism. Since the liver is fixed on its superior face to the diaphragm, the experiments consist in applying displacements to the superior surfacic nodes, the constraint of the ribs being active. The motion of the diaphragm is vertical, and is more important on its posterior side than on its anterior side [10] (fig.12 and fig.13).

Breathing depth	**Ant.**	**Post.**
shallow	5mm	14mm
deep	16mm	41mm

fig.12 - The behaviour of the diaphragm during breathing

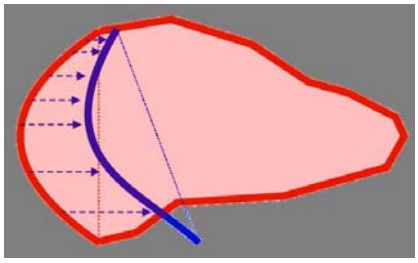

fig.13 – The behaviour of the diaphragm during breathing - illustration

Both deep and shallow breathing were simulated. The average motion of the nodes is 20.8mm ± 5.3mm in the first case, and 7.0mm ± 1.8mm in the second case. Although the protocols differ, as well as the tracked cloud of nodes, our measures match relatively well those found in [8] and [9]. Furthermore, the FE model can provide us with a 3D motion for a given set of nodes, which is useful to track the motion of the tumors.

5. CONCLUSION AND FUTURE WORK

This preliminary computational study of the motion and deformation of the liver is relatively satisfactory. We gathered information on tumor displacement while the radiofrequency needle is penetrating Glisson's capsule: some of the privileged segment-tumor directions lead to supra-millimetric displacements which should be taken into account for a future Computer Assisted Surgery System, and more specifically for the "trajectory planning" step. The movements of the global liver and of each tumor have been qualitatively evaluated as well.
Nevertheless, our model has to be enhanced for more precise and quantitative study. In a first step, the FE mesh will be modified: hexahedrons are preferred to tetrahedrons for FE simulations. Anisotropic structures such as the portal vein could be added into the mesh. Finally, the model will have to be patient-specific for an optimal preoperative planning (cf Luboz & al., current proceedings [11]).

6. REFERENCES

1. McGahan, J.P., Dodd, G.D., Radiofrequency Ablation of the Liver: Current Status, AJR 2001 ; 176:3-16.
2. Merloz, P., Tonetti, J., Cinquin, P., Lavallée, S., Troccaz, J., Pittet, L., Computer-assisted spine surgery, Computer Aided Surgery, 1998, 3:297-305
3. Voirin, D., Payan, Y., Amavizca, M., Leroy, A., Létoublon, C., Troccaz, J., Computer-Aided Hepatic Tumor Ablation : Requirements and Preliminary Results, Proceedings of the Fourth International Conference on Medical Image Computing and Computer-Assisted Interventions - MICCAI'2001, 1145-1146.
4. Dan, D., Caractérisation Mécanique du Foie Humain en Situation de Choc, PhD thesis, biomécanique, Université Paris VII, 1999
5. Carter, F. J., Franck, T.G., Davies, P.J., Cuschieri, A., Puncture Forces on Solid Organ Surfaces, Surgical Endoscopy, 2000, 14:783-786.
6. Ottensmeyer, M.P., Salisbury, J.K., In Vivo Data Acquisition Instrument for Solid Organ Mechanical Property Measurement, Proceedings of the Fourth International Conference on Medical Image Computing and Computer-Assisted Interventions - MICCAI'2001, 975-982.
7. Curley, S.A., Izzo, F., Delrio, P., Ellis, L.M., Granchi, J., Vallone, P., Fiore, F., Pignata, S., Daniele, B., Cremona, F., Radiofrequency Ablation of Unresectable Primary and Metastatic Hepatic Malignancies, Annals of Surgery, vol. 230, No 1, 1-8, 1999.
8. Herline, A.J., Herring, J.L., Stefansic, J.D., Chapman, W.C., Galloway, R.L., Davant, B.M., Surface Registration for Use in Interactive, Image-Guided Liver Surgery, Computer Aided Surgery, 2000, 5:11-17.
9. Schweikard, A., Glosser, G., Bodduluri, M., Murphy, M.J., Adler, J.R., Robotic Motion Compensation for Respiratory Movement during Radiosurgery, Computer Aided Surgery, 2000, 5:263-277.
10. Craighero, S., Imagerie Fonctionnelle du Diaphragme et de la Cage Thoracique Par IRM Dynamique en Echo Planar, MD thesis, médecine, Université Joseph Fourier, Grenoble, 2001.
11. Luboz, V. , Payan, Y., Swider, P., Couteau, B., Automatic 3D Finite Element Mesh Generation : Data Fitting for an Atlas, Proceedings of the Fifth International Symposium on Computer Methods in Biomechanics and Biomedical Engineering, BBE'2001.